NeuroImage: Clinical 21 (2019) 101631

Contents lists available at ScienceDirect

NeuroImage: Clinical

journal homepage: www.elsevier.com/locate/ynicl

Different patterns of white matter changes after successful surgery of mesial temporal lobe epilepsy

Wei Li[a,1], Dongmei An[a,1], Xin Tong[a], Wenyu Liu[a], Fenglai Xiao[a], Jiechuan Ren[a], Running Niu[b], Yingying Tang[a], Baiwan Zhou[b], Du Lei[b], Yuchao Jiang[c], Cheng Luo[c], Dezhong Yao[c], Qiyong Gong[b,**], Dong Zhou[a,*]

[a] Department of Neurology, West China Hospital, Sichuan University, Chengdu, Sichuan, China
[b] Huaxi MR Research Center, Department of Radiology, West China Hospital, Sichuan University, Chengdu, Sichuan, China
[c] Key Laboratory for NeuroInformation of Ministry of Education, Center for Information in Medicine, High-Field Magnetic Resonance Brain Imaging Key Laboratory of Sichuan Province, School of Life Science and Technology, University of Electronic Science and Technology of China, Chengdu, China.

ARTICLE INFO

Keywords:
Mesial temporal lobe epilepsy
Anterior temporal lobectomy
Hippocampal sclerosis
Diffusion tensor imaging
Reorganization

ABSTRACT

Objectives: To explore the dynamic changes of white matters following anterior temporal lobectomy (ATL) in mesial temporal lobe epilepsy (MTLE) patients who achieved seizure-free at two-year follow-up.
Methods: Diffusion tensor imaging (DTI) was obtained in ten MTLE patients at five serial time points: before surgery, three months, six months, 12 months and 24 months after surgery, as well as in 11 age- and sex-matched healthy controls at one time point. Regions with significant postoperative fractional anisotropy (FA) changes and their dynamic changes were confirmed by comparing all preoperative and postoperative data using Tract-Based Spatial Statistics (TBSS).
Results: After successful ATL, significant FA changes were found in widespread ipsilateral and contralateral white matter regions ($P < .05$, FWE correction). Ipsilateral external capsule, cingulum, superior corona radiate, body of corpus callosum, inferior longitudinal fasciculus, optic radiation and contralateral inferior cerebellar peduncle, inferior longitudinal fasciculus showed significant FA decrease at three months after surgery, without further changes. Ipsilateral superior cerebellar peduncle and contralateral corpus callosum, anterior corona radiate, external capsule, optic radiation showed significant FA decrease at three months follow up but increase later. Ipsilateral cerebral peduncle and contralateral middle cerebellar peduncle showed significant FA decrease at three months follow up, with further decrease after that. While ipsilateral posterior limb of internal capsule, retrolenticular part of internal capsule and contralateral posterior corona radiate showed significant FA increase after surgery.
Conclusions: FA changes after successful ATL presented as four distinct patterns, reflecting different structural adaptions following epilepsy surgery. Some FA increases indicated the reversibility of preoperative diffusion abnormalities and the possibility of structural reorganization, especially in the contralateral hemisphere.

1. Introduction

Mesial temporal lobe epilepsy (MTLE) is the most common medically intractable but surgically remediable type of epilepsy in adults (Kwan et al., 2011). Anterior temporal lobectomy (ATL) is a well-established treatment for refractory MTLE, with a seizure-free rate approximately of 60–70% (Wieser et al., 2001). Not only epileptic seizures but also other comorbidities, such as cognitive and emotional disorders, may be improved after surgery (Tanriverdi et al., 2010; Benuzzi et al., 2014). White matter changes in MTLE have been reported in many diffusion tensor imaging (DTI) studies, mainly reflected as fractional anisotropy (FA) reduction in ipsilateral temporal lobe white matters and extratemporal structures, such as the fornix, cingulum, external capsule and corpus callosum (Gross et al., 2006; Concha et al., 2009). These diffusion abnormalities may result from acute functional impairment induced by seizures and chronic structural changes (Concha

* Correspondence to: D. Zhou, Department of Neurology, West China Hospital, Sichuan University, Chengdu 610041, Sichuan, China.
** Correspondence to: Q. Gong, Huaxi MR Research Center, Department of Radiology, Center for Medical Imaging, West China Hospital, Sichuan University, Chengdu 610041, Sichuan, China.
E-mail addresses: qiyonggong@hmrrc.org.cn (Q. Gong), zhoudong66@yahoo.de (D. Zhou).
[1] These two authors contributed to this work equally.

https://doi.org/10.1016/j.nicl.2018.101631
Received 30 August 2018; Received in revised form 29 November 2018; Accepted 7 December 2018
Available online 08 December 2018

et al., 2007). It is known that the epileptic brain is structural reorganized after surgery, including white matters. Surgery directly impairs white matters through surgical axonal transection. Those white matter impairments induced by seizures may be reversible after surgery since seizures get stopped (Yasuda et al., 2009). However, the prognosis of those impairments induced by chronic structural changes is not well known. Furthermore, we cannot differentiate the causes of white matter changes before surgery. Therefore, exploring the white matter changes before and after the surgery can contribute to understanding the structural reorganization in epileptic brain and may help predicting postoperative outcome including seizure and other comorbidities (Keller et al., 2017; McDonald et al., 2010; Pustina et al., 2014; Taylor et al., 2018).

Extended FA reductions after surgery have been reported in tracts directly connected to the area of resection, such as ipsilateral fornix, uncinate fasciculus (UF), cingulum (CING) and inferior longitudinal fasciculus (ILF), which indicated the wallerian degeneration induced by surgical axonal transection (Concha et al., 2007; McDonald et al., 2010; Pustina et al., 2014; Faber et al., 2013; Schoene-Bake et al., 2009; Yogarajah et al., 2010; Nguyen et al., 2011; Winston et al., 2014; Liu et al., 2013). FA reductions have also been observed in some tracts indirectly connected to the resection zone, such as ipsilateral corpus callosum (CC), internal capsule (IC), external capsule (EC), superior longitudinal fasciculus (SLF), inferior fronto-occipital fasciculus (IFOF), posterior thalamic radiation (PTR) and even contralateral fornix, ILF, in which wallerian degeneration may also play an important role (Concha et al., 2007; McDonald et al., 2010; Pustina et al., 2014; Faber et al., 2013; Schoene-Bake et al., 2009; Yogarajah et al., 2010; Nguyen et al., 2011; Winston et al., 2014). However, only a few FA increases in ipsilateral IC, EC and corona radiate (CR) have been observed, suggesting the postoperative recovery of white matters (Pustina et al., 2014; Yogarajah et al., 2010; Winston et al., 2014). Recently, through white matter connectome analysis, it was found that resective epilepsy surgery may lead to increased contralateral axonal connectivity (Jeong et al., 2016) and the network change metrics may have clinical value for predicting seizure outcome (Taylor et al., 2018). In addition, findings in the dynamic diffusion changes of tracts over time are inconsistent. McDonald et al. (2010) found no additional FA decreases from two months to one year post-ATL, while Faber et al. (2013), on the contrary, found a significantly more widespread pattern of FA reduction in ipsilateral fornix and cingulum from 3 to 6 months to 12 months in left TLE. Besides, Winston et al. (2014) found little progression between 3 and 4 months and 12 months following surgery in left TLE, but more widespread changes in right TLE. These different findings may result from limited follow-up times and distinct patients and controls. Up to now, most studies have collected DTI data at one or two time points after surgery, with or without preoperative data and healthy controls, which may not completely reflect the dynamic changes of white matters before and after surgery. The sole DTI study with multiple postoperative scans only focused on the fornix at a very early period, from several days to four months following surgery, indicating FA reduced at the chronic stage (1–4 months) (Liu et al., 2013).

In this current study, we explored the longitudinal DTI changes in MTLE patients who achieved seizure-free after ATL at five serial time points: before surgery, three months, six months, 12 months and 24 months after surgery, aiming to depict the dynamic pictures of white matter changes following successful ATL.

2. Materials and methods

2.1. Participants

Patients were selected from the temporal lobe epilepsy database in West China Hospital. All patients were diagnosed with TLE according to the International League Against Epilepsy (ILAE) Classification Schemes of Epileptic Seizures and Epilepsy Syndromes (Engel, 2001) and underwent comprehensive preoperative evaluations at our multidisciplinary team consisted of epileptologists, neurosurgeons and radiologists. A combination of clinical symptom, ictal and interictal EEG, MRI and PET/CT was used to localize the seizure focus.

Thirty-two patients who underwent ATL at our center due to intractable MTLE were originally included into the study from April 2014 to December 2015. They were followed-up every three months after surgery for two years and surgical outcome was evaluated according to the ILAE classification (Wieser et al., 2001). DTI was scanned at five serial time points: before surgery, three months, six months, 12 months and 24 months after surgery, at our MR research center.

The inclusion criteria were as follows: (1) patients with intractable MTLE; (2) normal MRI or MRI evidence of hippocampal sclerosis (HS) ipsilateral to the lateralization by EEG; (3) no evidence of bilateral hippocampal sclerosis or of a secondary extrahippocampal lesion that may contribute to seizures; (4) reached favorable outcome (ILAE class 1) for at least two years; (5) underwent five serial DTI scans.

The exclusion criteria included: (1) patients with any other neurological disorder, psychiatric disorder, or serious systematic disease; (2) with alcohol or other substance abuse; (3) with other structural lesions except HS (according to ILAE classification (Blümcke et al., 2013)) confirmed by postoperative histopathological examination; (4) suffered persistent postoperative seizures; (5) lost to follow-up or failed to finish all five DTI scans.

At the end of follow-up, one patient who lost to follow-up, two patients with other structural lesions (hemangioma and focal cortical dysplasia, confirmed by postoperative histopathological examination) and 19 patients who failed to complete all five scans were excluded. Finally, only 10 patients (five right-sided and five left-sided) were enrolled in our study. All patients underwent ATL by one expert neurosurgeon using the same approach. In addition, we studied 11 age- and sex-matched healthy controls (4 males and 7 females, age range: 20–42 years) without any neurological or psychiatric disorders. They were only scanned at one time point. All participants were native Chinese speakers and were right-handed, as assessed by the Edinburgh Inventory handedness test.

This study was approved by the local ethics committee and informed consent was obtained from all participants.

2.2. Image acquisition

All DTI imaging was performed on a 3.0 T MRI system (Tim Trio; Siemens, Erlangen, Germany) with an eight-channel head coil. A spin-echo planar imaging sequence with the following parameters was used to obtain DTIs: repetition time (TR) = 6800 ms; echo time (TE) = 91 ms; matrix = 256 × 256; field of view (FOV) = 240 × 240 mm^2; slice thickness = 3 mm, no gap, 50 slices. The diffusion sensitizing gradients were applied along 64 non-collinear directions (b = 1000 s/mm^2) as well as a reference image with no diffusion weighting (b0 image). Participants were instructed to rest with their eyes closed and keep their heads still. Head motion was minimized by using foam pads.

2.3. Image processing

The diffusion maps were obtained using FSL (www.fmrib.ox.ac.uk/fsl) (Jenkinson et al., 2012). The eddy current distortions and head motion were corrected using FSL's “eddy current correction” (Jenkinson and Smith, 2001). Brain extraction was performed using the Brain Extraction Tool (BET) and FMRIB's Diffusion Toolbox (FDT) (Popescu et al., 2012; Behrens et al., 2003). Then, FA maps of all subjects were calculated in each voxel using DTIFIT (www.fmrib.ox.ac.uk/fsl/fdt/fdt_dtifit.html). The FA maps of right-side MTLE were left-right flipped to obtain ipsilateral and contralateral datasets. A sub-sample of HC, age- and gender- matched with patients, was selected to left-right flipped according to an in-house group matching algorithm (Supekar et al.,

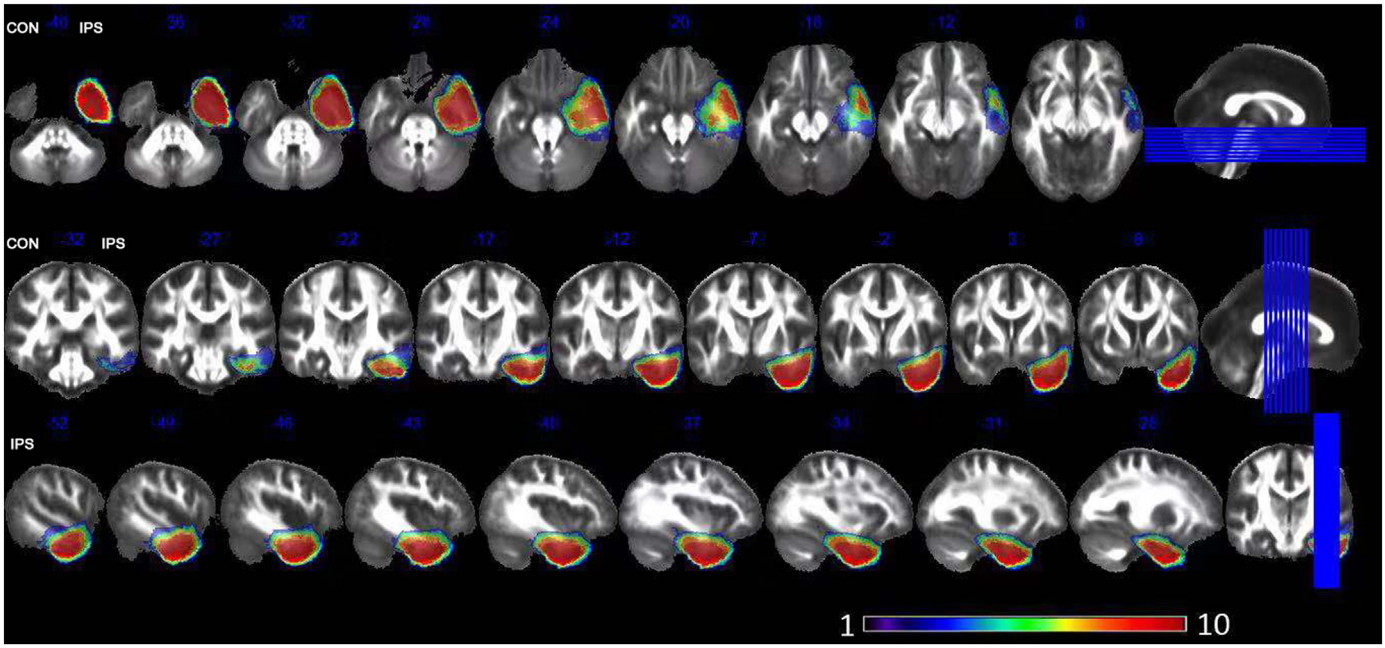

Fig. 1. Surgical resections. The color bar from purple to red represents as voxel was directly affected by surgery in one patient to 10 patients. Purple areas indicate the voxels only affected in one patient and red areas indicate the voxels affected in all 10 patients. CON: contralateral; IPS: ipsilateral.

2018). The FA maps of HC and preoperative MTLE subjects were nonlinearly normalized to standard space and then averaged to obtain a group mean standard template. Subsequently, the mean template was left-to-right flipped and re-averaged to create a symmetrical template (Zuo et al., 2010; Zhang et al., 2017; Vaughan et al., 2017). Preoperative FA map from individual native space was nonlinearly registered to the symmetrical template. And each postoperative image was registered to the corresponding preoperative image using affine registration, and then nonlinearly normalized to the symmetrical template with the surgical resection as a mask to eliminate the information from resected areas (Winston et al., 2014). The surgical resections (Fig. 1) were manually delineated by overlaying the postoperative high resolution T1 images on the preoperative T1 images to have the idea of what is missing. The final decision was based on the agreement of the two investigators (Li W and An D). If there was discrepancy, a third opinion was acquired (Zhou D).The agreement rate between our two investigators was about 90%, which was defined as the mean overlap rate of their manually delineated resected regions.

2.4. Statistical analysis

The first step was the whole brain voxel-wised analysis using Tract-Based Spatial Statistics (TBSS) method. The normalized FA images were thinned to create a skeleton, and each subject's FA map was projected to the skeleton. The resulting data were used for voxel-wise repeated measured ANCOVA with age and gender as covariates. In addition, each patient's resection mask was also registered into common space by applying the normalization approach mentioned as above. These masks were averaged and a further threshold at 10% was set to create a group resection mask to remove voxels in statistical analysis (Winston et al., 2014). Multiple comparison correction was performed using the Threshold-Free Cluster Enhancement method (Winkler et al., 2016; Smith and Nichols, 2009). A family-wise error corrected $P < .05$ was considered statistically significant.

The second step was the specific fiber tracts analysis. Those regions with significant FA difference from repeated measured ANCOVA were extracted at each time point to calculate their mean FA values. For plotting their dynamic FA changes, post-hoc paired *t*-test was used to compare the FA difference between any two of the five time points (before surgery, three months, six months, 12 months and 24 months after surgery). $P < .005$ was considered as a corrected significance through Bonferroni correction because of the comparison between five time points.

Furthermore, independent-samples t-test was used to compare the FA differences of these regions between preoperative data of patients and data of controls.

3. Results

3.1. Clinical data

Seven of the 10 patients were female. The median age at surgery was 27 years old (range: 19–39). The median duration of epilepsy was 13 years (range: 4–26 years). All patients had at least one focal seizure per month before surgery, with or without secondary generalized tonic-clonic seizures. All patients underwent unilateral ATL (five/five, L/R) and achieved ILAE class 1 after surgery for at least two years. The median follow-up time was 35 months (range: 25–43 months). Antiepileptic medications in the first two years after surgery remained the same as those prior to surgery for all patients. Hippocampal sclerosis (HS) was confirmed by postoperative histopathological test in five patients and gliosis only was found in the other five patients. Detailed clinical and demographic information of the patients were summarized in Table 1.

There was no statistically significant difference in age, gender, race and handedness between patients and healthy controls.

3.2. Postoperative FA changes

3.2.1. Whole-brain voxel-wise analysis

Results of whole-brain voxel-wise TBSS analysis comparing FA maps of patients between all preoperative and postoperative data using repeated measured ANCOVA were showed in Table 2. Significant FA changes were observed in widespread white matter regions outside the resected areas after surgery ($P < .005$) (Fig. 2).

3.2.2. Specific fiber tracts analysis

The mean FA values of aforementioned regions in control group and

Table 1
Clinical characteristics of TLE patients.

Subject	Sex	Age at surgery (year)	Handedness	Course of disease (year)	Seizure type	Seizure frequency (no/mon)	Seizure focus	Pathology (ILAE classification)	Postop seizure outcome (ILAE classification)
1	F	25	Right	16	FS, SGTC(rare)	6	L	gliosis	Class 1
2	F	38	Right	26	FS	5	R	gliosis	Class 1
3	M	27	Right	20	FS, SGTC(rare)	1	L	gliosis	Class 1
4	M	20	Right	14	FS, SGTC	2	R	HS type 1	Class 1
5	M	20	Right	4	FS, SGTC	6	L	HS type 1	Class 1
6	F	26	Right	9	FS, SGTC(rare)	60	L	HS type 1	Class 1
7	F	26	Right	6	FS, SGTC	30	L	gliosis	Class 1
8	F	33	Right	18	FS	3	R	gliosis	Class 1
9	F	19	Right	12	FS	5	R	HS type 2	Class 1
10	F	39	Right	8	FS	13	R	HS type 1	Class 1

F: female; M: male; FS: focal seizure; SGTC: secondary generalized tonic-clonic seizure; L: left; R: right; HS: hippocampal sclerosis; TLE: temporal lobe epilepsy; ILAE: International League Against Epilepsy.

patient group at each time point were presented in Table 3. Compared with control group, ipsilateral posterior limb of internal capsule (PLIC-I), body of corpus callosum (BCC-I), inferior longitidinal fasciculus (ILF-I) and contralateral genu of corpus callosum (GCC-C), anterior corona radiate (ACR-C), posterior corona radiate (PCR-C), optic radiation (OR-C) showed significant FA reduction before surgery ($P < .05$).

Comparisons of FA between any two of the five time points in patient group were presented in Table 4. Compared among the five time-points in patients, postoperative FA in these tracts changed in four different patterns (Fig. 3): (1) ipsilateral external capsule (EC-I), cingulum (CING-I), superior corona radiate (SCR-I), body of corpus callosum (BCC-I), inferior longitudinal fasciculus (ILF-I), optic radiation (OR-I) and contralateral inferior cerebellar peduncle (ICP-C), inferior longitudinal fasciculus (ILF-C) showed significant FA decrease at three months after surgery, without further changes (Fig. 3A); (2) ipsilateral superior cerebellar peduncle (SCP-I) and contralateral body of corpus callosum (BCC-C), genu of corpus callosum (GCC-C), splenium of corpus callosum (SCC-C), anterior corona radiate (ACR-C), external capsule (EC-C), optic radiation (OR-C) showed significant FA reduction at 3-month after surgery, but later significant increase at some point (Fig. 3B): SCP-I, BCC-C and EC-C showed significant FA increase from 6 to 12 months, GCC-C showed significant FA increase from 3 to 24 months, SCC-C showed significant FA increase from 12 to 24 months, ACR-C showed significant FA increase from 6 to 24 months, OR-C showed significant FA increase from 3 to 12 months; (3) ipsilateral cerebral peduncle (CP-I) and contralateral middle cerebellar peduncle (MCP-C) showed significant FA decreased at three months post-ATL, with further decrease after that (Fig. 3C): CP-I showed significant FA decrease from 3 to 24 months and MCP-C showed significant FA decrease from 3 to 6 months; (4) ipsilateral posterior limb of internal capsule (PLIC-I), retrolenticular part of internal capsule (RIC-I) and contralateral posterior corona radiate (PCR-C) showed significant FA increase after surgery (Fig. 3D): PLIC-I showed significant FA increase from 6 months; RIC-I and PCR-C showed significant FA increase from 3 months.

Fig. 3A represented FA significantly decreased at three months after surgery and remained relatively stable; Fig. 3B represented FA significantly reduced at three months but then increased at some point (SCP-I, BCC-C and EC-C showed significant FA increase from 6 to 12 months; GCC-C showed significant FA increase from 3 to 24 months; SCC-C showed significant FA increase from 12 to 24 months; ACR-C showed significant FA increase from 6 to 24 months; OR-C showed significant FA increase from 3 to 12 months); Fig. 3C represented FA significantly decreased at three months, with further decrease after that (CP-I showed significant FA decrease from 3 to 24 months and MCP-C showed significant FA decrease from 3 to 6 months); Fig. 3D represented FA significantly increased after surgery (PLIC-I showed significant FA increase from 6 months; RIC-I and PCR-C showed significant FA increase from 3 months).

4. Discussion

The current study explored the dynamic white matter changes following ATL at five serial time points: before surgery, three months, six

Table 2
Results of comparing FA maps of patients between all preoperative and postoperative data using voxel-wise repeated measured ANCOVA.

Region	Abbreviation	X	Y	Z	F value	Cluster size
Contralateral middle cerebellar peduncle	MCP-C	26	−69	−39	22.2	300
Contralateral inferior cerebellar peduncle	ICP-C	12	−46	−30	23.3	209
Contralateral external capsule	EC-C	29	−6	18	54.15	261
Contralateral splenium of corpus callosum	SCC-C	21	−42	26	22.1	3984
Contralateral body of corpus callosum	BCC-C	16	−16	35	7.06	3984
Contralateral genu of corpus callosum	GCC-C	16	26	21	15.85	3984
Contralateral anterior corona radiate	ACR-C	27	29	13	15.23	175
Contralateral posterior corona radiate	PCR-C	25	−26	33	6.96	3984
Contralateral inferior longitudinal fasciculus	ILF-C	38	−28	10	45.5	382
Contralateral optic radiation	OR-C	28	−65	16	13.47	3984
Ipsilateral superior cerebellar peduncle	SCP-I	−7	−33	−19	16.96	9939
Ipsilateral cerebral peduncle	CP-I	−17	−20	−9	33.64	9939
Ipsilateral external capsule	EC-I	−29	9	−11	22.6	9939
Ipsilateral posterior limb of internal capsule	PLIC-I	−24	−7	16	9.81	9939
Ipsilateral retrolenticular part of internal capsule	RIC-I	−29	−30	11	14.94	9939
Ipsilateral cingulum	CING-I	−7	−11	35	12.63	138
Ipsilateral superior corona radiate	SCR-I	−18	−22	35	9.49	1182
Ipsilateral body of corpus callosum	BCC-I	−6	−22	25	16.68	1182
Ipsilateral inferior longitudinal fasciculus	ILF-I	−29	−16	−9	14.38	9939
Ipsilateral optic radiation	OR-I	−28	−66	1	17.63	9939

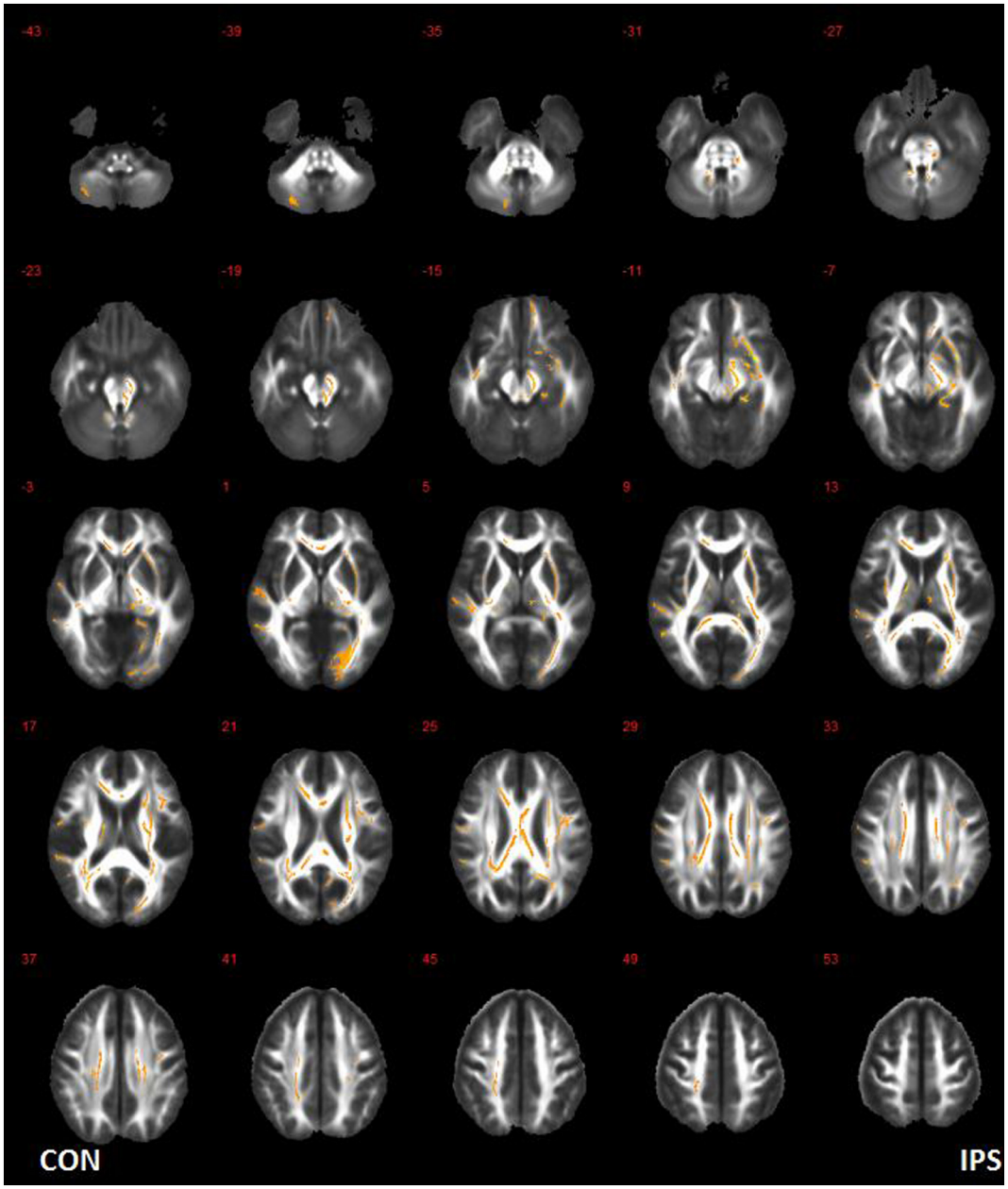

Fig. 2. White matter regions with significant postoperative FA changes. CON: contralateral hemisphere; IPS: ipsilateral hemisphere.

months, 12 months and 24 months after surgery in MTLE patients who achieved seizure-free at two-year follow-up. In addition, 11 age- and sex-matched healthy controls were scanned at one time point for comparison. We found significant FA changes after surgery in widespread ipsilateral and contralateral regions, including ipsilateral CING, IC, cerebral peduncle and bilateral EC, CR, CC, ILF, OR, cerebellar peduncle ($P < .05$, FWE correction). There were no significant FA changes in these regions before surgery except FA decreases in ipsilateral PLIC, BCC, ILF and contralateral GCC, ACR, PCR, OR ($P < .05$). Furthermore, it is interesting that we found four distinct types of FA changes after ATL, including (1) FA decreased at three months and remained relatively stable; (2) FA decreased at three months but increased later; (3) FA decreased at three months, with further decrease after that; (4) FA increased after surgery. These findings may illustrate the complicacy and variability of structural reorganization in epileptic brains.

DTI can effectively assess white matters in vivo. FA describes the variance between the levels of diffusion measured in three different directions, reflecting fiber density, axonal diameter and myelination in white matters (Mori and Zhang, 2006). FA can be affected by many factors, such as changes in intra- and extra-cellular volume, permeability of cell membranes, fiber coherence, axonal loss, mechanical stretch and degeneration of crossing fibers (Beaulieu, 2002). Baseline FA reduction in ipsilateral PLIC, BCC, ILF and contralateral GCC, ACR, PCR, OR was in line with most previous studies and was thought to be the result of impaired myelination, altered membrane permeability or neuronal packing density, induced by uncontrolled seizures or chronic structural changes (Concha et al., 2007; Winston et al., 2014; Song et al., 2003). More importantly, four different patterns of postoperative white matter changes were demonstrated in the current study from 3-month to 2-year after ATL. This is the first study to explore FA changes before and after ATL at so many time points in such a long period.

In the first three patterns, we observed significant FA decreases from three months after surgery in ipsilateral CING, EC, SCR, BCC, ILF, OR, CP and contralateral EC, ACR, CC, ILF, OR, MCP, ICP. Postoperative FA reductions have been previously reported in tracts directly and

Table 3
Mean FA of white matter regions with significant postoperative changes.

Region	HC	Pre	3-mon	6-mon	12-mon	24-mon
MCP-C	0.3246 ± 0.0738	0.3280 ± 0.0617	0.2413 ± 0.0304	0.2273 ± 0.0240	0.2210 ± 0.0270	0.2439 ± 0.0371
ICP-C	0.6242 ± 0.0672	0.5672 ± 0.0669	0.4854 ± 0.0617	0.4829 ± 0.0582	0.4882 ± 0.0734	0.5001 ± 0.0550
EC-C	0.5676 ± 0.0425	0.5518 ± 0.0441	0.4764 ± 0.0364	0.4730 ± 0.0333	0.4915 ± 0.0393	0.4858 ± 0.0370
SCC-C	0.5739 ± 0.0365	0.5715 ± 0.0530	0.4984 ± 0.0489	0.4991 ± 0.0432	0.4896 ± 0.0413	0.5099 ± 0.0416
BCC-C	0.5621 ± 0.0871	0.5735 ± 0.0622	0.5227 ± 0.0627	0.5002 ± 0.0660	0.5419 ± 0.0541	0.5315 ± 0.0577
GCC-C	0.6576 ± 0.0408	0.5813 ± 0.0513	0.5053 ± 0.0549	0.5166 ± 0.0481	0.5233 ± 0.0471	0.5305 ± 0.0375
ACR-C	0.4954 ± 0.0416	0.4498 ± 0.0379	0.3683 ± 0.0333	0.3622 ± 0.0174	0.3756 ± 0.0456	0.3811 ± 0.0372
PCR-C	0.4526 ± 0.0464	0.3769 ± 0.0500	0.4035 ± 0.0447	0.3986 ± 0.0472	0.4050 ± 0.0451	0.4119 ± 0.0465
ILF-C	0.4942 ± 0.0357	0.4587 ± 0.0363	0.3505 ± 0.0492	0.3534 ± 0.0515	0.3614 ± 0.0552	0.3561 ± 0.0572
OR-C	0.7855 ± 0.0386	0.7349 ± 0.0597	0.6485 ± 0.0893	0.6582 ± 0.0812	0.6717 ± 0.0874	0.6614 ± 0.0962
SCP-I	0.7918 ± 0.0471	0.7884 ± 0.0503	0.6772 ± 0.0366	0.6738 ± 0.0393	0.7040 ± 0.0450	0.7063 ± 0.0661
CP-I	0.7792 ± 0.0243	0.7581 ± 0.0445	0.6401 ± 0.0489	0.6180 ± 0.0418	0.6109 ± 0.0673	0.6065 ± 0.0602
EC-I	0.5397 ± 0.0664	0.4875 ± 0.0695	0.3155 ± 0.0525	0.3045 ± 0.0553	0.3156 ± 0.0595	0.3167 ± 0.0663
PLIC-I	0.5982 ± 0.0314	0.5594 ± 0.0416	0.5783 ± 0.0551	0.6040 ± 0.0503	0.6194 ± 0.0381	0.6196 ± 0.0401
RIC-I	0.5951 ± 0.0532	0.5607 ± 0.0490	0.6098 ± 0.0498	0.6089 ± 0.0471	0.6345 ± 0.0337	0.6366 ± 0.0292
CING-I	0.5886 ± 0.0820	0.5686 ± 0.0893	0.4559 ± 0.0713	0.4649 ± 0.0809	0.4588 ± 0.0735	0.4772 ± 0.1115
SCR-I	0.5202 ± 0.0673	0.5156 ± 0.0674	0.4364 ± 0.0673	0.4308 ± 0.0754	0.4482 ± 0.0797	0.4475 ± 0.0757
BCC-I	0.7591 ± 0.0278	0.7229 ± 0.0486	0.6222 ± 0.0566	0.6016 ± 0.0511	0.6146 ± 0.0650	0.6238 ± 0.0416
ILF-I	0.5308 ± 0.0773	0.4397 ± 0.0546	0.3573 ± 0.0433	0.3576 ± 0.0461	0.3386 ± 0.0502	0.3600 ± 0.0502
OR-I	0.5681 ± 0.0887	0.5106 ± 0.0763	0.3964 ± 0.0895	0.4039 ± 0.0536	0.4325 ± 0.0747	0.4143 ± 0.0781

HC: healthy controls; Pre: pre-surgery; 3-mon: 3 months after surgery; 6-mon: 6 months after surgery; 12-mon: 12 months after surgery; 24-mon: 24 months after surgery; MCP-C: contralateral middle cerebellar peduncle; ICP-C: contralateral inferior cerebellar peduncle; EC-C: contralateral external capsule; SCC-C: contralateral splenium of corpus callosum; BCC-C: contralateral body of corpus callosum; GCC-C: contralateral genu of corpus callosum; ACR-C: contralateral anterior corona radiate; PCR-C: contralateral posterior corona radiate; ILF-C: contralateral inferior longitudinal fasciculus; OR-C: contralateral optic radiation; SCP-I: ipsilateral superior cerebellar peduncle; CP-I: ipsilateral cerebral peduncle; EC-I: ipsilateral external capsule; PLIC-I: ipsilateral posterior limb of internal capsule; RIC-I: ipsilateral retrolenticular part of internal capsule; CING-I: ipsilateral cingulum; SCR-I: ipsilateral superior corona radiate; BCC-I: ipsilateral body of corpus callosum; ILF-I: ipsilateral inferior longitudinal fasciculus; OR-I: ipsilateral optic radiation.

indirectly connected to the resection area, mostly in the first year after surgery (Concha et al., 2007; McDonald et al., 2010; Faber et al., 2013; Yogarajah et al., 2010; Nguyen et al., 2011; Winston et al., 2014; Liu et al., 2013), except one after 3–11 years (Schoene-Bake et al., 2009). Similar FA reductions in ipsilateral CING were found in many DTI studies (Concha et al., 2007; McDonald et al., 2010; Schoene-Bake et al., 2009; Faber et al., 2013; Winston et al., 2014). Following directly surgical axonal transection, downstream Wallerian degeneration leads to FA reduction in ipsilateral CING. Previous studies have also reported reduced FA in EC, CR, CC, ILF, OR and CP (Concha et al., 2007; McDonald et al., 2010; Schoene-Bake et al., 2009; Yogarajah et al., 2010; Winston et al., 2014). Although not directly transected in surgery, fibers in these regions were more or less interconnected with temporal lobe and also affected by Wallerian degeneration after ATL (Yogarajah et al., 2010).

However, regarding their dynamic FA changes from three to

Table 4
Comparison of FA (T value) between different time points (**P < .005, *P < .05).

Region	3-mon/Pre	6-mon/Pre	12-mon/Pre	24-mon/Pre	6-mon/3-mon	12-mon/3-mon	24-mon/3-mon	12-mon/6-mon	24-mon/6-mon	24-mon/12-mon
EC-I	−11.75**	−6.27**	−6.95**	−5.05**	−0.54	−0.00	0.04	0.63	0.58	0.08
CING-I	−7.62**	−7.27**	−5.24**	−4.25**	0.58	0.18	0.85	−0.55	0.55	0.81
SCR-I	−4.77**	−5.98**	−3.21*	−3.81**	−0.55	0.67	0.57	1.36	1.28	−0.07
BCC-I	−8.88**	−8.95**	−4.92**	−6.61**	−1.42	−0.35	0.09	0.71	1.29	0.61
ILF-I	−4.45**	−3.97**	−4.91**	−5.30**	0.01	−1.58	0.28	−1.25	0.20	2.04
OR-I	−7.19**	−8.34**	−6.68**	−7.92**	0.43	1.91	0.87	1.93	0.58	−1.75
ICP-C	−7.32**	−8.96**	−6.36**	−6.30**	−0.29	0.29	1.53	0.63	1.75	0.98
ILF-C	−10.48**	−9.53**	−10.89**	−8.43**	0.34	1.19	0.49	1.01	0.40	−0.61
SCP-I	−7.74**	−9.96**	−8.55**	−4.57**	−0.29	1.59	1.25	3.07*	1.48	0.14
BCC-C	−3.31*	−3.91**	−2.10	−3.34*	−2.54*	1.52	0.60	3.34*	1.80	−0.83
GCC-C	−7.07**	−4.74**	−6.20**	−3.78**	1.38	1.98	2.88*	0.64	1.39	1.74
SCC-C	−5.50**	−6.83**	−6.95**	−4.27**	0.11	−1.34	1.56	−1.44	1.15	2.43*
ACR-C	−5.71**	−7.45**	−3.78**	−4.14**	−0.62	0.62	0.99	1.27	2.44*	0.63
EC-C	−10.74**	−9.67**	−12.00**	−8.90**	−0.55	2.26	1.44	3.51*	2.59*	−1.37
OR-C	−6.62**	−5.81**	−4.15**	−3.64*	1.06	2.53*	0.78	1.46	0.27	−0.96
CP-I	−8.27**	−8.66**	−9.00**	−8.45**	−1.80	−1.65	−3.16*	−0.51	−0.72	−0.24
MCP-C	−4.82**	−6.20**	−5.74**	−4.54**	−2.40*	−1.84	0.27	−0.93	1.81	1.83
PLIC-I	1.15	3.23*	5.36**	4.24**	3.43*	4.45**	2.95*	1.74	1.19	0.02
RIC-I	3.49*	3.48*	5.76**	6.95**	−0.13	2.06	2.80*	2.09	3.22*	0.21
PCR-C	3.44*	2.85*	3.64*	4.30**	−1.00	0.19	0.97	1.21	1.66	1.44

Pre: pre-surgery; 3-mon: 3 months after surgery; 6-mon: 6 months after surgery; 12-mon: 12 months after surgery; 24-mon: 24 months after surgery; EC-I: ipsilateral external capsule; CING-I: ipsilateral cingulum; SCR-I: ipsilateral superior corona radiate; BCC-I: ipsilateral body of corpus callosum; ILF-I: ipsilateral inferior longitudinal fasciculus; OR-I: ipsilateral optic radiation; ICP-C: contralateral inferior cerebellar peduncle; ILF-C: contralateral inferior longitudinal fasciculus; SCP-I: ipsilateral superior cerebellar peduncle; BCC-C: contralateral body of corpus callosum; GCC-C: contralateral genu of corpus callosum; SCC-C: contralateral splenium of corpus callosum; ACR-C: contralateral anterior corona radiate; EC-C: contralateral external capsule; OR-C: contralateral optic radiation; CP-I: ipsilateral cerebral peduncle; MCP-C: contralateral middle cerebellar peduncle; PLIC-I: ipsilateral posterior limb of internal capsule; RIC-I: ipsilateral retrolenticular part of internal capsule; PCR-C: contralateral posterior corona radiate.

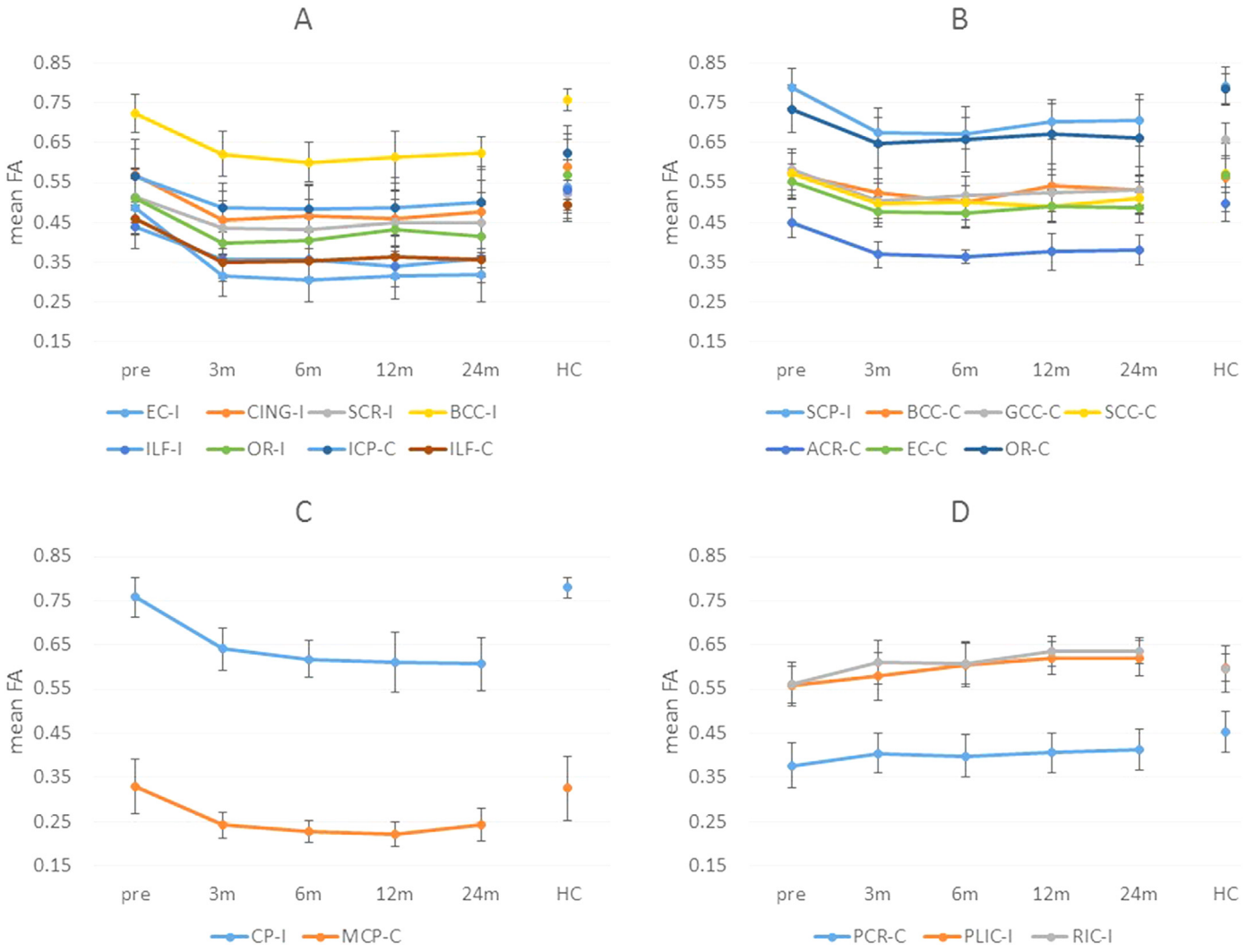

Fig. 3. Different FA changes after surgery. Y-axis: mean FA value; X-axis: different time point; pre: pre-surgery; 3 m: 3 months after surgery; 6 m: 6 months after surgery; 12 m: 12 months after surgery; 24 m: 24 months after surgery. EC-I: ipsilateral external capsule; CING-I: ipsilateral cingulum; SCR-I: ipsilateral superior corona radiate; BCC-I: ipsilateral body of corpus callosum; ILF-I: ipsilateral inferior longitudinal fasciculus; OR-I: ipsilateral optic radiation; ICP-C: contralateral inferior cerebellar peduncle; ILF-C: contralateral inferior longitudinal fasciculus; SCP-I: ipsilateral superior cerebellar peduncle; BCC-C: contralateral body of corpus callosum; GCC-C: contralateral genu of corpus callosum; SCC-C: contralateral splenium of corpus callosum; ACR-C: contralateral anterior corona radiate; EC-C: contralateral external capsule; OR-C: contralateral optic radiation; CP-I: ipsilateral cerebral peduncle; MCP-C: contralateral middle cerebellar peduncle; PCR-C: contralateral posterior corona radiate; PLIC-I: ipsilateral posterior limb of internal capsule; RIC-I: ipsilateral retrolenticular part of internal capsule.

24 months, we found three different changing trends. In our pattern A, FA in ipsilateral CING, EC, SCR, BCC, ILF, OR and contralateral ICP, ILF remained relatively stable, without further changes. In our pattern B, FA in ipsilateral SCP and contralateral CC, ACR, EC, OR increased at some latter time point. While in our pattern C, FA in ipsilateral CP and contralateral MCP further decreased after three months. Three published studies have tried to assess the dynamic diffusion changes of tracts over time. However, they only acquired the postoperative DTI data at two time points and their findings were not consistent. McDonald et al. (2010) found no additional FA decreases from two months to one year post-ATL, which was similar to our pattern A and compatible with myelin degradation and slow clearance of axonal and myelin debris, lasting from 1 to 4 months to years (Liu et al., 2013; Vargas and Barres, 2007). Faber et al. (2013), on the contrary, found a significantly more widespread pattern of FA reduction from 3 to 6 months to 12 months, which was similar to our pattern C. But they only included patients with left TLE who acquired selective amygdalohippocampectomy (SAH) and the groups at 3–6 months and 12 months were not the same, which limited our further comparison. Besides, Winston et al. (2014) found little progression between 3 and 4 months and 12 months following ATL in left TLE, but more widespread changes in right TLE. However, they only visually compared the ranges of FA changes, without direct comparison of FA values between these two time points, thus failed to find the latter FA increase in our pattern B. The significant decrease and latter increase of FA mainly in contralateral CC, ACR, EC, and OR may reflect the reversible influence of seizures and surgery to contralateral hemisphere.

In the fourth pattern, we observed significant FA increase after surgery in ipsilateral PLIC, RIC and contralateral PCR. Furthermore, ipsilateral PLIC and RIC even showed a further FA increase from 3 to 24 months. FA increases in ipsilateral IC were observed in two previous studies, actually from one group, however, Yogarajah et al. (2010) only found FA increase at 4-month after surgery, and Winston et al. (2014) found more marked changes in right TLE from 3 to 4 months to 12 months. Increases in FA were mostly thought to be related to the structural plasticity after surgery, not only in language networks, but also in memory system and other aspects (Yogarajah et al., 2010; Nguyen et al., 2011; Winston et al., 2014; Eacott and Gaffan, 2005). Similar recovery has been found in some MR spectroscopy or PET studies in epilepsy, and the ability of structural reorganization has also

been reported in human brains and animal models after injury (Lantz et al., 2006; Ramu et al., 2008; Jain et al., 2000). It's worth noting that our FA in ipsilateral PLIC and RIC increased to a level higher than healthy controls. There has been a debate on the cause. Pustina et al. (2014) attributed the abnormally high FA to degeneration of crossing fibers. But Winston et al. (2014) thought the inference of crossing fibers seemed less likely in IC since their fibers were expected to be more coherent. In this study, increased FA were also found in contralateral PCR, which remained relatively stable from 3 to 24 months and didn't exceed the level of healthy controls at the end of follow up. There shouldn't be degeneration of crossing fibers in contralateral hemisphere. Moreover, FA increase in contralateral CR has also been reported in one study after hemispherectomy, which in turn indicated the genuine neuroplastic response (Govindan et al., 2013). Up to now, although researchers have tried to adopt other diffusion parameters, such as mean diffusivity (MD), radial diffusivity (RD), parallel diffusivity (PD) or mode of anisotropy (MO) to further confirm the interference of crossing fibers, it is still an unresolved problem in DTI studies (Pustina et al., 2014; Winston et al., 2014). It seems arbitrary to simply attribute FA increases in ipsilateral PLIC and RIC to either structural reorganization or degeneration of crossing fibers. But the FA increase in contralateral PCR did indicate the reversibility of preoperative FA reduction and the possibility of structural reorganization.

Although this was a very preliminary study including a small group of 10 seizure-free patients, but even in this small group, different patterns of diffusion changes before and after ATL were demonstrated, reflecting the diversity and complicacy of brain structural adaption. These changes may be related to different clinical status, e.g. seizure control, cognitive performance etc. Some FA increases we observed do indicate the reversibility of preoperative diffusion abnormalities and the possibility of structural reorganization, which may be the benefit of epilepsy surgery except for seizure-control. Hopefully, the pattern of diffusion changes may have a predictive value in terms of seizure control, relapse, cognitive improvement or deterioration etc. In addition, FA increases mainly in the contralateral regions indicate the contralateral hemisphere may play an important role in postoperative recovery, which may become a diffusion marker for predicting outcomes of epilepsy surgery.

4.1. Limitations

The current study has several limitations that need to be addressed. Firstly, since we only recruited patients with all five serial DTI data, the sample size was small, which may limit the power of the statistical analysis. Secondly, we flipped DTI images to combine analysis, which may interfere with the results because of differences between left and right hemisphere and between left-sided ATL and right-sided ATL. We have attempted to minimize the influences by adopting a symmetrical template. And further studies with larger sample size may allow analyze the changes in each hemisphere independently. Thirdly, all our findings in FA changes were observed on a group level. It is convincing but difficult to observe consistent results in each patient. Finally, neuropsychological tests were not included for correlation with diffusion changes, which need further studies enrolling larger group of patients to clarify.

5. Conclusion

FA changes after successful ATL presented as four distinct patterns, reflecting different structural adaptions following epilepsy surgery. Some FA increases indicated the reversibility of preoperative diffusion abnormalities and the possibility of structural reorganization, especially in the contralateral hemisphere.

Disclosures

Authors have no conflicts of interest to declare.

Acknowledgements

This study was supported by NSFC Grant No.81401079, 81771402 and 81401076. We wish to thank the staff of the department of radiology for their collaboration and assistance. And we are grateful to all our subjects and colleagues for their enthusiastic cooperation.

Appendix A. Supplementary data

Supplementary data to this article can be found online at https://doi.org/10.1016/j.nicl.2018.101631.

References

Beaulieu, C., 2002. The basis of anisotropic water diffusion in the nervous system - a technical review. NMR Biomed. 15, 435–455.
Behrens, T.E., Woolrich, M.W., Jenkinson, M., et al., 2003. Characterization and propagation of uncertainty in diffusion-weighted MR imaging. Magn. Reson. Med. 50 (5), 1077–1088.
Benuzzi, F., Zamboni, G., Meletti, S., et al., 2014. Recovery from emotion recognition impairment after temporal lobectomy. Front. Neurol. 5, 92.
Blümcke, I., Thom, M., Aronica, E., et al., 2013. International consensus classification of hippocampal sclerosis in temporal lobe epilepsy: a task force report from the ILAE commission on diagnostic methods. Epilepsia 54 (7), 1315–1329.
Concha, L., Beaulieu, C., Wheatley, B.M., et al., 2007. Bilateral white matter diffusion changes persist after epilepsy surgery. Epilepsia 48 (5), 931–940.
Concha, L., Beaulieu, C., Collins, D.L., et al., 2009. White-matter diffusion abnormalities in temporal-lobe epilepsy with and without mesial temporal sclerosis. J. Neurol. Neurosurg. Psychiatry 80 (3), 312–319.
Eacott, M.J., Gaffan, E.A., 2005. The roles of perirhinal cortex, postrhinal cortex, and the fornix in memory for objects, contexts, and events in the rat. Q. J. Exp. Psychol. B 58 (3–4), 202–217.
Engel, J., 2001. A proposed diagnostic scheme for people with epileptic seizures and with epilepsy: report of the ILAE task force on classification and terminology. Epilepsia 42 (6), 796–803.
Faber, J., Schoene-Bake, J.C., Trautner, P., et al., 2013. Progressive fiber tract affections after temporal lobe surgery. Epilepsia 54 (4), e53–e57.
Govindan, R.M., Brescoll, J., Chugani, H.T., 2013. Cerebellar pathway changes following cerebral hemispherectomy. J. Child Neurol. 28 (12), 1548–1554.
Gross, D.W., Concha, L., Beaulieu, C., 2006. Extratemporal white matter abnormalities in mesial temporal lobe epilepsy demonstrated with diffusion tensor imaging. Epilepsia 47 (8), 1360–1363.
Jain, N., Florence, S.L., Qi, H.X., et al., 2000. Growth of new brainstem connec-tions in adult monkeys with massive sensory loss. Proc. Natl. Acad. Sci. U. S. A. 97 (10), 5546–5550.
Jenkinson, M., Smith, S., 2001. A global optimisation method for robust affine registration of brain images. Med. Image Anal. 5 (2), 143–156.
Jenkinson, M., Beckmann, C.F., Behrens, T.E.J., et al., 2012. Fsl. NeuroImage 62 (2), 782–790.
Jeong, J.W., Asano, E., Juhász, C., et al., 2016. Postoperative axonal changes in the contralateral hemisphere in children with medically refractory epilepsy: a longitudinal diffusion tensor imaging connectome analysis. Hum. Brain Mapp. 37 (11), 3946–3956.
Keller, S.S., Glenn, G.R., Weber, B., et al., 2017. Preoperative automated fibre quantification predicts postoperative seizure outcome in temporal lobe epilepsy. Brain 140 (1), 68–82.
Kwan, P., Schachter, S.C., Brodie, M.J., 2011. Drug-resistant epilepsy. N. Engl. J. Med. 365, 919–926.
Lantz, G., Seeck, M., Lazeyras, F., 2006. Extent of preoperative abnormalities and focus lateralization predict postoperative normalization of contralateral 1H-magnetic resonance spectroscopy metabolite levels in patients with temporal lobe epilepsy. AJNR Am. J. Neuroradiol. 27 (8), 1766–1769.
Liu, M., Gross, D.W., Wheatley, B.M., et al., 2013. The acute phase of Wallerian degeneration: longitudinal diffusion tensor imaging of the fornix following temporal lobe surgery. NeuroImage 74, 128–139.
McDonald, C.R., Hagler, D.J., Girard, H.M., et al., 2010. Changes in fiber tract integrity and visual fields after anterior temporal lobectomy. Neurology 75 (18), 1631–1638.
Mori, S., Zhang, J., 2006. Principles of diffusion tensor imaging and its applications to basic neuroscience research. Neuron 51 (5), 527–539.
Nguyen, D., Vargas, M.I., Khaw, N., et al., 2011. Diffusion tensor imaging analysis with tract-based spatial statistics of the white matter abnormalities after epilepsy surgery. Epilepsy Res. 94 (3), 189–197.
Popescu, V., Battaglini, M., Hoogstrate, W.S., et al., 2012. Optimizing parameter choice for FSL-brain extraction tool (BET) on 3D T1 images in multiple sclerosis. NeuroImage 61 (4), 1484–1494.
Pustina, D., Doucet, G., Evans, J., et al., 2014. Distinct types of white matter changes are

observed after anterior temporal lobectomy in epilepsy. PLoS One 9 (8), e104211.
Ramu, J., Herrera, J., Grill, R., et al., 2008. Brain fiber tract plasticity in experimental spinal cord injury: diffusion tensor imaging. Exp. Neurol. 212 (1), 100–107.
Schoene-Bake, J.C., Faber, J., Trautner, P., et al., 2009. Widespread affections of large fiber tracts in postoperative temporal lobe epilepsy. NeuroImage 46 (3), 569–576.
Smith, S.M., Nichols, T.E., 2009. Threshold-free cluster enhancement: addressing problems of smoothing, threshold dependence and localisation in cluster inference. NeuroImage 44 (1), 83–98.
Song, S.K., Sun, S.W., Ju, W.K., et al., 2003. Diffusion tensor imaging detects and differentiates axon and myelin degeneration in mouse optic nerve after retinal ischemia. NeuroImage 20, 1714–1722.
Supekar, K., Cai, W., Krishnadas, R., et al., 2018. Dysregulated brain dynamics in a triple-network saliency model of schizophrenia and its relation to psychosis. Biol. Psychiatry S0006-3223 (18) (31715-3).
Tanriverdi, T., Dudley, R.W., Hasan, A., et al., 2010. Memory outcome after temporal lobe epilepsy surgery: corticoamygdalohippocampectomy versus selective amygdalohippocampectomy. J. Neurosurg. 113 (6), 1164–1175.
Taylor, P.N., Sinha, N., Wang, Y., et al., 2018. The impact of epilepsy surgery on the structural connectome and its relation to outcome. NeuroImage 18, 202–214.
Vargas, M.E., Barres, B.A., 2007. Why is Wallerian degeneration in the CNS so slow? Annu. Rev. Neurosci. 30, 3153–3179.
Vaughan, D.N., Raffelt, D., Curwood, E., et al., 2017. Tract-specific atrophy in focal epilepsy: disease, genetics, or seizures? Ann. Neurol. 81 (2), 240–250.
Wieser, H.G., Blume, W.T., Fish, D., et al., 2001. ILAE commission report. Proposal for a new classification of outcome with respect to epileptic seizures following epilepsy surgery. Epilepsia 42 (2), 282–286.
Winkler, A.M., Ridgway, G.R., Douaud, G., et al., 2016. Faster permutation inference in brain imaging. NeuroImage 141, 502–516.
Winston, G.P., Stretton, J., Sidhu, M.K., et al., 2014. Progressive white matter changes following anterior temporal lobe resection for epilepsy. Neuroimage 4, 190–200.
Yasuda, C.L., Valise, C., Saúde, A.V., et al., 2009. Dynamic changes in white and gray matter volume are associated with outcome of surgical treatment in temporal lobe epilepsy. NeuroImage 49 (1), 71–79.
Yogarajah, M., Focke, N.K., Bonelli, S.B., et al., 2010. The structural plasticity of white matter networks following anterior temporal lobe resection. Brain 133 (Pt 8), 2348–2364.
Zhang, Z., Liao, W., Xu, Q., et al., 2017. Hippocampus-associated causal network of structural covariance measuring structural damage progression in temporal lobe epilepsy. Hum. Brain Mapp. 38 (2), 753–766.
Zuo, X.N., Kelly, C., Di Martino, A., et al., 2010. Growing together and growing apart: regional and sex differences in the lifespan developmental trajectories of functional homotopy. J. Neurosci. 30 (45), 15034–15043.